

Southern Illinois University Carbondale OpenSIUC

Publications

Department of Physics

3-2013

Enhancement of Ferromagnetism by Cr Doping in Ni-Mn-Cr-Sb Heusler Alloys

Mahmud Khan
University of Alberta

Igor Dubenko
Southern Illinois University Carbondale

Shane Stadler
Louisiana State University

J. Jung
University of Alberta

S. S. Stoyko
University of Alberta

See next page for additional authors

Follow this and additional works at: http://opensiuc.lib.siu.edu/phys_pubs

© 2013 American Institute of Physics

Published in *Applied Physics Letters* Vol. 102 No. 112402 (2013) at doi: [10.1063/1.4795627](https://doi.org/10.1063/1.4795627)

Recommended Citation

Khan, Mahmud, Dubenko, Igor, Stadler, Shane, Jung, J., Stoyko, S. S., Mar, Arthur, Quetz, Abdiel, Samanta, Tampas, Ali, Naushad and Chow, K. H. "Enhancement of Ferromagnetism by Cr Doping in Ni-Mn-Cr-Sb Heusler Alloys." (Mar 2013).

This Article is brought to you for free and open access by the Department of Physics at OpenSIUC. It has been accepted for inclusion in Publications by an authorized administrator of OpenSIUC. For more information, please contact opensiuc@lib.siu.edu.

Authors

Mahmud Khan, Igor Dubenko, Shane Stadler, J. Jung, S. S. Stoyko, Arthur Mar, Abdiel Quetz, Tampas Samanta, Naushad Ali, and K. H. Chow

Enhancement of ferromagnetism by Cr doping in Ni-Mn-Cr-Sb Heusler alloys

Mahmud Khan,¹ Igor Dubenko,² Shane Stadler,³ J. Jung,¹ S. S. Stoyko,⁴ Arthur Mar,⁴ Abdiel Quetz,² Tapas Samanta,² Naushad Ali,² and K. H. Chow¹

¹Department of Physics, University of Alberta, Edmonton, Alberta T6G 2E1, Canada

²Department of Physics, Southern Illinois University Carbondale, Carbondale, Illinois 62901, USA

³Department of Physics and Astronomy, Louisiana State University, Baton Rouge, Louisiana 70803, USA

⁴Department of Chemistry, University of Alberta, Edmonton, Alberta T6G 2G2, Canada

(Received 15 September 2012; accepted 4 March 2013; published online 18 March 2013)

A series of Mn rich $\text{Ni}_{50}\text{Mn}_{37-x}\text{Cr}_x\text{Sb}_{13}$ Heusler alloys have been investigated by dc magnetization and electrical resistivity measurements. Due to the weakening of the Ni-Mn hybridization, the martensitic transition shifts to lower temperatures with increasing Cr concentration, while the saturation magnetization at 5 K increases. The magnetoresistance and exchange bias properties are dramatically suppressed with increasing Cr concentration. The observed behaviors suggest that substitution of Cr for Mn in $\text{Ni}_{50}\text{Mn}_{37-x}\text{Cr}_x\text{Sb}_{13}$ Heusler alloys not only destabilizes the martensitic phase but also enhances ferromagnetism in the system. The possible mechanisms responsible for the observed behavior are discussed. © 2013 American Institute of Physics. [<http://dx.doi.org/10.1063/1.4795627>]

Since their discovery in 1903, Heusler alloys¹ have been a subject of intense research interest due to the diverse magnetic properties they exhibit. These ternary intermetallic alloys have the general formula XYZ (called Half- or semi-Heusler) or X_2YZ (full Heusler alloys), in which X and Y typically are transition metals and Z is a main group element. Both of these Heusler alloy families exhibit cubic structures with four interpenetrating FCC sublattices. X_2YZ (also expressed as $X_{50}Y_{25}Z_{25}$) crystallize in the $L2_1$ structure where two of the sublattices are occupied by the X -atoms. The XYZ Heusler alloys exhibit the $C1_b$ structure where one X -atom sublattice remains unoccupied. Further details are available in, e.g., Ref. 2.

Among the full Heusler alloys, Ni_2MnGa is perhaps the most well known because it undergoes a martensitic phase transition at 202 K, during which the high temperature $L2_1$ phase (austenite) of the alloy transforms to a low temperature phase (martensite) with a lower symmetry. In the martensitic phase, the alloy exhibits ferromagnetic shape memory properties.³ Currently, a series of Mn rich $\text{Ni}_{50}\text{Mn}_{50-y}\text{Z}_y$ ($Z = \text{In}, \text{Sb}, \text{Sn}$) Heusler alloys are also being paid extensive attention because they also exhibit martensitic phase transitions.⁵⁻⁹ In the vicinity of the transition, large magnetocaloric effects,³ large magnetoresistance, and exchange bias effects are observed.⁴ Unlike Ni_2MnGa , where both the martensitic and austenitic phases are ferromagnetic, both antiferromagnetism and ferromagnetism exist in the martensitic phase of these Mn rich Heusler alloys, whereas the austenite exhibits ferromagnetic correlations.¹⁰ While this coexistence of different magnetic interactions in the martensitic phase results in the observation of exchange bias behavior,^{11,12} the change of magnetism during the martensitic phase transition results in the observation of large magnetic entropy changes^{6,13} and magnetoresistance.^{14,15} Thus, the multifunctional properties of the $\text{Ni}_{50}\text{Mn}_{50-y}\text{Z}_y$ Heusler alloys not only depend on the martensitic phase transition but also depend strongly on the strengths of the magnetic interactions in the two phases.

It has been recently shown that the hybridization between the Ni atoms and the Mn atoms on the Z sites is

an important driving force for the martensitic transformation in Mn-rich Ni-Mn-Z full Heusler alloys.¹⁶⁻¹⁸ Based on the results of first-principles calculations and extended x-ray absorption fine structure (EXAFS) studies of Ni-Mn-In full Heusler alloys, it has also been suggested that the Ni-Mn hybridization may be responsible for the magnetic properties, especially the antiferromagnetic interactions in the martensitic state, of the alloys.^{18,19} According to these suggestions, a stronger hybridization would result in a stronger antiferromagnetic exchange and a weaker hybridization would imply a weaker antiferromagnetic exchange. Thus, the net ferromagnetism of the alloy would be enhanced with the weakening of the hybridization. Recently, we showed that partial replacement of Mn by Cr in $\text{Ni}_{50}\text{Mn}_{37-x}\text{Cr}_x\text{Sb}_{13}$ Heusler alloys results in the destabilization of the martensitic phase due to the weakening of the Ni-Mn hybridization.¹⁵ From both scientific and applied points of view, it is interesting to explore how the magnetic properties of these alloys change with Cr substitution. If the strength of the Ni-Mn hybridization really plays a dominant role in influencing the magnetism of these alloys, Cr substitution is expected to weaken the antiferromagnetic (AFM) interactions of the martensitic phase and strengthen the net ferromagnetism of $\text{Ni}_{50}\text{Mn}_{37-x}\text{Cr}_x\text{Sb}_{13}$ alloys. Such an observation would provide a strong indication that not only does the strength of Ni-Mn hybridization determine the AFM interactions in Ni-Mn-In based Heusler alloys, as suggested in Refs. 14 and 15, but that it is in fact universally applicable to all Mn rich Ni-Mn-Z Heusler alloys.

Keeping in mind the above discussion, in this letter, we report experimental investigations of a series of $\text{Ni}_{50}\text{Mn}_{37-x}\text{Cr}_x\text{Sb}_{13}$ Heusler alloys. We performed dc magnetization and electrical resistivity measurements on the samples and evaluated the magnetic entropy changes, exchange bias effects, and magnetoresistance. Our experimental observations strongly suggest that Cr substitution suppresses the AFM interactions in the $\text{Ni}_{50}\text{Mn}_{37-x}\text{Cr}_x\text{Sb}_{13}$ alloys, resulting in the enhancement of ferromagnetism.

The alloys were prepared by conventional arc-melting in an argon atmosphere. The details regarding the sample preparation and the structural properties of the samples may be found in Ref. 17. The dc magnetization measurements were performed using a superconducting quantum interference device (SQUID) manufactured by Quantum Design, Inc. The measurements were performed in a temperature range of 10–400 K and in magnetic fields up to 50 kOe. Direct current (DC) resistivity, using the four-probe method, was measured over the same temperature range as the magnetization measurements. To eliminate the contribution of thermoelectric effects, the current direction was reversed and an average of the voltage drops in each direction was recorded.

Figure 1 shows the magnetization as a function of increasing temperature, $M(T)$, of selected $\text{Ni}_{50}\text{Mn}_{37-x}\text{Cr}_x\text{Sb}_{13}$ alloys. The procedure for zero-field-cooled (ZFC) and field-cooled heating (FCH) measurements may be found in Ref. 17. The ZFC $M(T)$ data of the alloy with $x=0$ exhibit three transitions (see Fig. 1(a)) that are typically observed in these alloys.^{8,9} The exchange bias blocking temperature, T_{EB} , was observed at 74 K followed by the martensitic transition temperature, T_M at 293 K and the ferromagnetic transition temperature of the austenitic phase, T_C^A at 342 K. As usual, due to pinning effects, T_{EB} was only observed in the ZFC $M(T)$ data. As Mn was initially replaced by a small amount of Cr ($x=1$), an additional transition (ferromagnetic transition temperature, T_C^M , of the martensitic phase) was observed in the alloy, while T_M shifted to higher temperature. As x exceeds 1, T_M decreases with increasing Cr, while T_C^M is no longer observed in the alloys (see Figs. 1(c) and 1(d)).

Figure 2 shows the $M(T)$ of selected $\text{Ni}_{50}\text{Mn}_{37-x}\text{Cr}_x\text{Sb}_{13}$ alloys measured at a magnetic field of 50 kOe. The thermal hysteresis observed in the $M(T)$ data obtained while cooling and warming signifies the first order nature of the martensitic transition. For the sample with $x=1$, the magnetization decreases with increasing temperature as the sample approaches T_C^M , followed by a sharp increase at T_M . With increasing temperature, the magnetization of the samples with higher concentration of Cr decreases at a relatively slower rate

due to the fact that the samples do not exhibit T_C^M . It is also to be noted that, with increasing Cr concentration, the magnitude of the magnetization change at T_M decreases for the alloys, and for the alloy with $x=5$, any change in magnetization at T_M is hardly noticeable (see upper inset of Fig. 2). In Mn rich Heusler alloys, the change in magnetization at T_M is attributed to the suppression of the AFM interactions of the martensitic phase during the phase transition.

As shown in the lower inset of Fig. 2, the saturation moment M_S at 5 K (martensitic phase), estimated by extrapolation of magnetization curves $M(H)$ at 5 K to infinite magnetic field, of $\text{Ni}_{50}\text{Mn}_{37-x}\text{Cr}_x\text{Sb}_{13}$ alloy increases with increasing Cr concentration, which demonstrates the enhancement of FM interactions and the suppression of the AFM interaction. Since the AFM interactions are already diminished in the martensitic phase due to Cr substitution, the relative change of the AFM interactions to FM interactions at T_M is smaller, and hence the magnitude of the magnetization change at T_M decreases with increasing Cr concentration.

The reduction of AFM interactions of the martensitic phase of $\text{Ni}_{50}\text{Mn}_{37-x}\text{Cr}_x\text{Sb}_{13}$ alloys is also reflected in the decrease of T_{EB} with increasing Cr concentration (see Fig. 3(a)). The magnitude of the corresponding shift of the magnetic hysteresis loop and the coercive field obtained under field cooled condition (EB effects) also reduces with increasing Cr concentration (see Figs. 3(b)–3(e)). The EB effect²⁰ is an interface effect between AFM and FM regions of the martensitic phase.²¹ A reduction in the AFM interactions makes it difficult for the AFM region to pin the domains of the FM region, and hence a reduction in the EB effects is observed.

This supports the claim that Cr substitution does reduce the AFM interactions in the $\text{Ni}_{50}\text{Mn}_{37-x}\text{Cr}_x\text{Sb}_{13}$ alloys. The magnetic entropy changes, ΔS_M , as a function of temperature (evaluated from the isothermal magnetization data using Maxwell Relation²⁵) of the alloy with $x=1$, are shown in Fig. 3(f). For $\Delta H=50$ kOe, peak values of ≈ 20 J/kg K in the vicinity of T_M and ≈ 13 J/kg K in the vicinity of T_C^A are observed in the data. The large peak value of ΔS_M observed

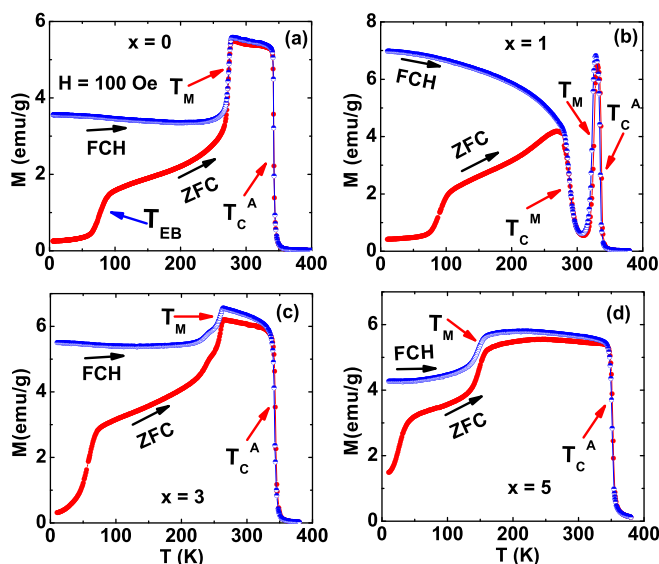


FIG. 1. Magnetization as a function of increasing temperature of selected $\text{Ni}_{50}\text{Mn}_{37-x}\text{Cr}_x\text{Sb}_{13}$ alloys measured at a magnetic field of 100 Oe.

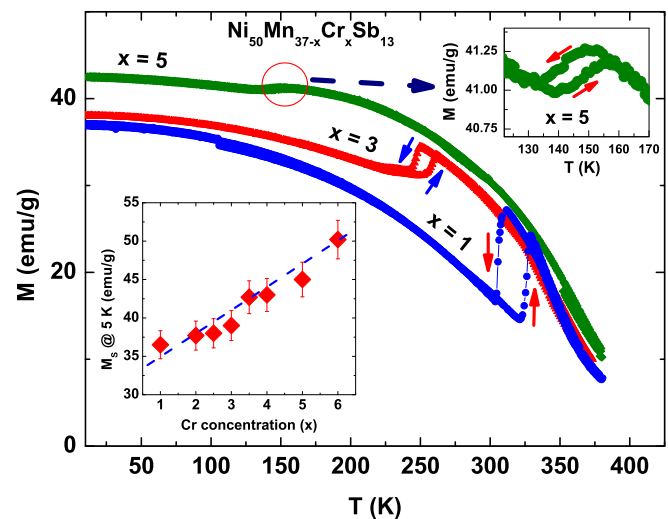


FIG. 2. Magnetization as a function of increasing temperature of selected $\text{Ni}_{50}\text{Mn}_{37-x}\text{Cr}_x\text{Sb}_{13}$ alloys measured in an applied magnetic field of 50 kOe. The upper inset shows the $M(T)$ data for the alloy with $x=5$ in the vicinity of the martensitic transition. The lower inset shows the saturation magnetic moment at 5 K as a function of Cr concentration.

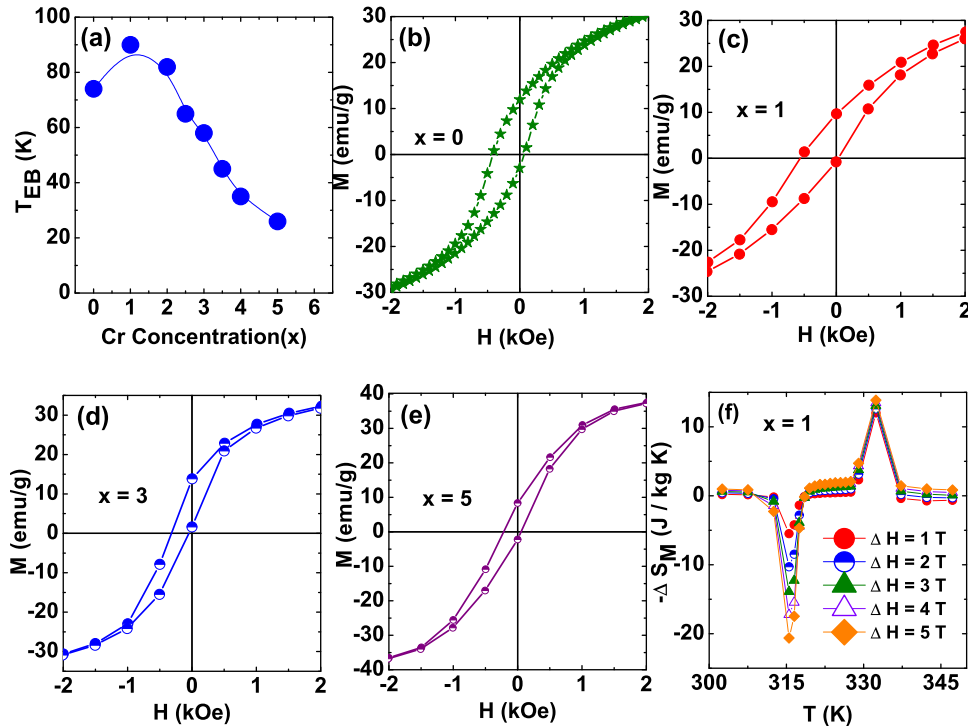


FIG. 3. (a) The exchange bias transition temperature as a function of Cr concentration. (b)–(e) Field cooled hysteresis loops of selected $\text{Ni}_{50}\text{Mn}_{37-x}\text{Cr}_x\text{Sb}_{13}$ alloys measured at 5 K. (f) The magnetic entropy change (ΔS_M) as a function of temperature of the $\text{Ni}_{50}\text{Mn}_{37-x}\text{Cr}_x\text{Sb}_{13}$ ($x = 1$).

near T_M is typical for these alloys, and the alloy with $x = 0$ also exhibit similar behavior.¹³ However, the value of $\approx 13 \text{ J/kg K}$ observed near T_C^A is unusual since the transition at T_C^A is a second order transition. It is possible that since $T_M (=325 \text{ K})$ and $T_C^A (=337 \text{ K})$ in the $\text{Ni}_{50}\text{Mn}_{37-x}\text{Cr}_x\text{Sb}_{13}$ alloy with $x = 1$ are very close, a partial martensitic transformation also occurs at T_C^A , and hence, the large ΔS_M peak is observed near T_C^A . The magnetocaloric effect in Mn rich Heusler alloys is associated with the magnitude of the magnetization change at T_M . As shown in Fig. 2, this magnitude decreases dramatically with increasing Cr concentration due to the enhancement of ferromagnetism of the martensitic phase. Therefore, significantly smaller ΔS_M is expected for the alloys with higher Cr concentration.

The temperature dependence of the electrical resistivity, $\rho(T)$, obtained while cooling and warming for the $\text{Ni}_{50}\text{Mn}_{37-x}\text{Cr}_x\text{Sb}_{13}$ alloy with $x = 1$ is shown in Fig. 4(a). The inset of the Fig. 4(a) shows the $\rho(T)$ for the same alloy measured at 0 and 50 kOe magnetic fields. A sharp drop in resistivity was observed in the vicinity of T_M , which is a typical signature of a martensitic transition in Mn-rich Ni-Mn-Z Heusler alloys. A slope change in the $\rho(T)$ data represents the T_C^A (see Fig. 4(a)). The alloy with $x = 0$ exhibits similar behavior as reported in Ref. 4. As shown in the inset of Fig. 4(a), the application of a 50 kOe dc magnetic field lowers the T_M , which is also typical for these alloys. This drop of T_M upon the application of a magnetic field results in large magnetoresistance ($\text{MR} = 100 \times (\rho(0) - \rho(H))/\rho(0)$), and the MR of selected alloys are shown in Fig. 4(b). For the alloys with $x = 1$, a peak MR of $\approx 12\%$ was observed, and the peak MR decreases significantly with increasing Cr concentration. In intermetallic compounds, including the Mn rich Heusler alloys, that exhibit a phase transition involving a change of AFM interactions, the sharp change of resistivity in the vicinity of the phase transition (T_M in case of Heusler alloys) is a result of the formation of a super-zone gap. Due to

the establishment of the AFM sublattice, the underlying zone boundaries get redefined giving rise to a gap at the Fermi level. The conduction electrons thus have to overcome this gap, resulting in a large anomaly in the transport properties.^{22–24}

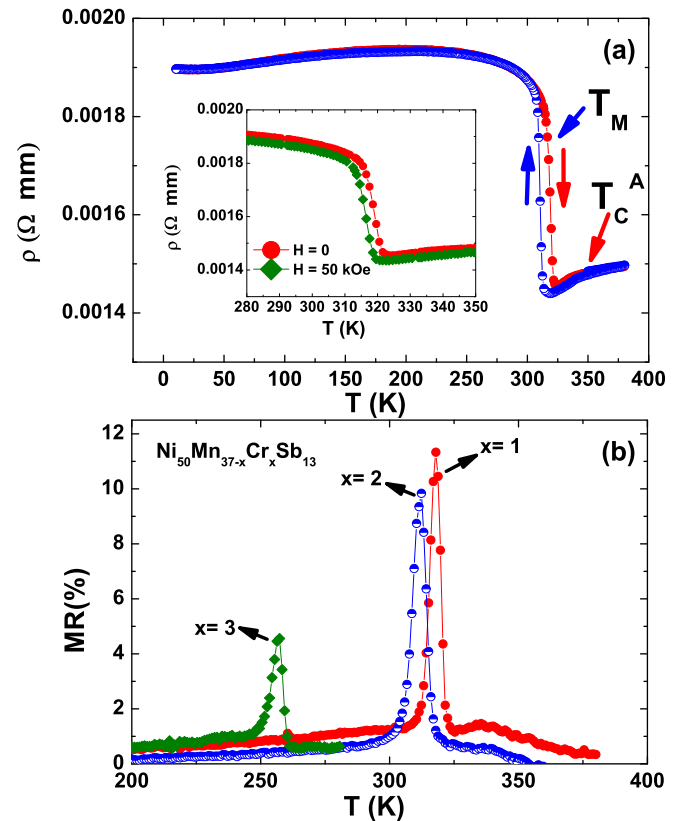


FIG. 4. (a) Electrical resistivity as a function of increasing and decreasing temperature of $\text{Ni}_{50}\text{Mn}_{37-x}\text{Cr}_x\text{Sb}_{13}$ ($x = 1$). The inset shows the resistivity data measured while warming in the vicinity of the martensitic transition for 0 and 50 kOe applied magnetic fields. (b) Magnetoresistance for a field change of 50 kOe of selected $\text{Ni}_{50}\text{Mn}_{37-x}\text{Cr}_x\text{Sb}_{13}$ alloys.

Therefore, the sharp drop of resistivity at T_M , the lowering of T_M with applied magnetic field, and the related MR in Mn-rich Ni-Mn-Z Heusler alloys are strongly dependent on the strength of the AFM interactions of the martensitic phase. The decreases of MR with increasing Cr concentration reflects the weakening of the AFM interactions in the martensitic phase, which is consistent with the observations in the magnetization data shown in Figs. 2 and 3.

The experimental results presented above clearly demonstrate that Cr substitution in $\text{Ni}_{50}\text{Mn}_{37-x}\text{Cr}_x\text{Sb}_{13}$ alloys suppresses the AFM interactions and enhances the resultant FM interactions in the alloys. Priolkar *et al.*¹⁹ and Tan *et al.*¹⁸ recently suggested that the AFM interactions in the martensitic phase of Mn rich Ni-Mn-Z alloys arise mainly due to the hybridization between the Ni atoms and the Mn atoms on the Z sites. The strength of this hybridization is strongly influenced by the Ni-Mn distance. Therefore, a question arises: how does Cr doping affect this Ni-Mn distance in $\text{Ni}_{50}\text{Mn}_{37-x}\text{Cr}_x\text{Sb}_{13}$ alloys? Considering coordination number, $\text{CN} = 12$, and depending on the number of electrons contributed to the conduction band when combined with other metals, Mn and Cr may have different metallic radii. For a valency of 3 and 6, the radii for Cr are 1.36 Å and 1.282 Å, respectively. The radii for Mn are 1.304 Å and 1.264 Å depending on the valency of 4 and 6, respectively.²⁶ Therefore, it is possible that the radius of Cr in $\text{Ni}_{50}\text{Mn}_{37-x}\text{Cr}_x\text{Sb}_{13}$ could be either smaller or larger than Mn. As shown in Fig. 5, the cell volume of the $\text{Ni}_{50}\text{Mn}_{37-x}\text{Cr}_x\text{Sb}_{13}$ system tends to increase with increasing Cr concentration. This implies that the radius of Cr is larger than that of Mn (Ni-Mn distance is larger). At this point, a question may arise regarding the possibility of Cr occupying the Ni sites. If this possibility is considered, even then the cell volume and the corresponding Ni-Mn distance will increase as the metallic radius of Ni (1.246 Å) is smaller than both radii of Cr. In light of above discussion, it can be concluded that the increase in the Ni-Mn distance, and corresponding weakening of Ni-Mn hybridization, is the main reason behind the enhancement of ferromagnetism in $\text{Ni}_{50}\text{Mn}_{37-x}\text{Cr}_x\text{Sb}_{13}$ alloys.

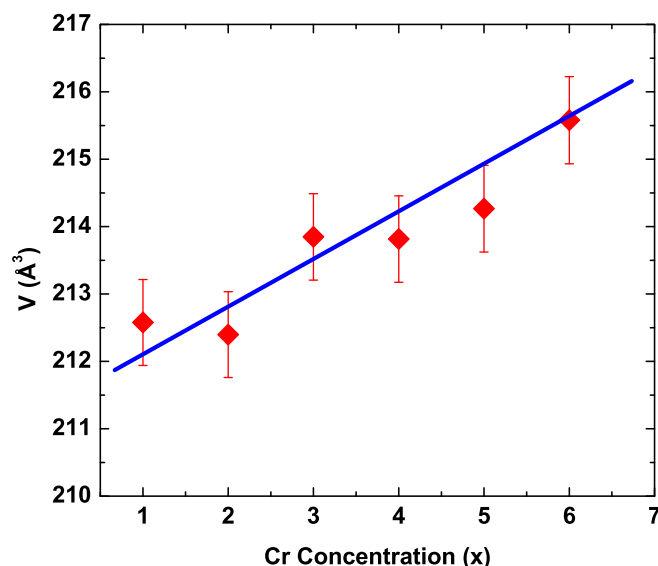


FIG. 5. The room temperature cell volume of $\text{Ni}_{50}\text{Mn}_{37-x}\text{Cr}_x\text{Sb}_{13}$ alloys as a function of Cr concentration.

In summary, we have investigated the magnetic, structural, and transport properties of $\text{Ni}_{50}\text{Mn}_{37-x}\text{Cr}_x\text{Sb}_{13}$ Heusler alloys. With increasing Cr concentration, suppression of AFM interactions and enhancement of the FM interactions were observed. These changes in the magnetic exchange interactions are reflected in the magnetic properties, including exchange bias and magnetoresistance. The experimental observations suggest that Cr substitution in $\text{Ni}_{50}\text{Mn}_{37-x}\text{Cr}_x\text{Sb}_{13}$ alloys weakens the Ni-Mn hybridization, which not only destabilizes the martensitic phase transition in the alloys but also enhances the resultant ferromagnetism.

This work was supported by the Natural Sciences and Engineering Research Council of Canada. The authors (Mahmud Khan) also acknowledge the support of the Killam Trusts at the University of Alberta. The part of the work conducted at Southern Illinois University and Louisiana State University was supported by the Office of Basic Energy Sciences, Material Science Division of the U.S. Department of Energy (Grant No. DE-FG02-06ER46291).

¹F. Heusler, Verh. Dtsch. Phys. Ges. **5**, 219 (1903).

²T. Graf, S. S. P. Parkin, and C. Felser, *IEEE Trans. Magn.* **47**, 367 (2011).

³A. Planes, L. Manosa, and M. Acet, *J. Phys.: Condens. Matter* **21**, 233201 (2009).

⁴V. D. Buchelnikov and V. V. Sokolovskiy, *Phys. Met. Metallogr.* **112**, 633 (2011).

⁵T. Krenke, M. Acet, E. F. Wassermann, X. Moya, L. Mañosa, and A. Planes, *Phys. Rev. B* **72**, 014412 (2005).

⁶T. Krenke, M. Acet, E. F. Wassermann, X. Moya, L. Mañosa, and A. Planes, *Nature Mater.* **4**, 450 (2005).

⁷T. Krenke, M. Acet, E. F. Wassermann, X. Moya, L. Mañosa, and A. Planes, *Phys. Rev. B* **73**, 174413 (2006).

⁸M. Khan, I. Dubenko, S. Stadler, and N. Ali, *J. Phys. Condens. Matter* **20**, 235204 (2008).

⁹S. E. Muthu, N. V. R. Rao, M. M. Raja, D. M. R. Kumar, D. M. Radheep, and S. Arumugam, *J. Phys. D: Appl. Phys.* **43**, 425002 (2010).

¹⁰S. Aksoy, M. Acet, P. P. Deen, L. Mañosa, and A. Planes, *Phys. Rev. B* **79**, 212401 (2009).

¹¹M. Khan, I. Dubenko, S. Stadler, and N. Ali, *Appl. Phys. Lett.* **91**, 072510 (2007).

¹²B. M. Wang, Y. Liu, P. Ren, B. Xia, K. B. Ruan, J. B. Yi, J. Ding, X. G. Li, and L. Wang, *Phys. Rev. Lett.* **106**, 077203 (2011).

¹³M. Khan, N. Ali, and S. Stadler, *J. Appl. Phys.* **101**, 053919 (2007).

¹⁴A. K. Pathak, I. Dubenko, C. Pueblo, S. Stadler, and N. Ali, *Appl. Phys. Lett.* **96**, 172503 (2010).

¹⁵M. Khan, A. K. Pathak, M. R. Paudel, I. Dubenko, S. Stadler, and N. Ali, *J. Magn. Magn. Mater.* **320**, L21–L25 (2008).

¹⁶M. Ye, A. Kimura, Y. Miura, M. Shirai, Y. T. Cui, K. Shimada, H. Namatame, M. Taniguchi, S. Ueda, K. Kobayashi, R. Kainuma, T. Shishido, K. Fukushima, and T. Kanomata, *Phys. Rev. Lett.* **104**, 176401 (2010).

¹⁷M. Khan, J. Jung, S. S. Stoyko, A. Mar, A. Quetz, T. Samanta, I. Dubenko, N. Ali, S. Stadler, and K. H. Chow, *Appl. Phys. Lett.* **100**, 172403 (2012).

¹⁸C. L. Tan, Y. W. Huang, X. H. Tian, J. X. Jiang, and W. Cai, *Appl. Phys. Lett.* **100**, 132402 (2012).

¹⁹K. R. Priolkar, D. N. Lobo, P. A. Bhoje, S. Emura, and A. K. Niga, *Europhys. Lett.* **94**, 38006 (2011).

²⁰J. Nogués and I. K. Schuller, *J. Magn. Magn. Mater.* **192**, 203 (1999).

²¹S. Giri, M. Patra, and S. Majumdar, *J. Phys.: Condens. Matter* **23**, 073201 (2011).

²²V. Sechovsky, L. Havela, K. Prokes, H. Nakotte, F. R. Deboer, and E. Bruck, *J. Appl. Phys.* **76**, 6913 (1994).

²³V. N. Antonov, A. Y. Perlov, P. M. Oppeneer, A. N. Yaresko, and S. V. Halilov, *Phys. Rev. Lett.* **77**, 5253 (1996).

²⁴B. Zhang, X. X. Zhang, S. Y. Yu, J. L. Chen, Z. X. Cao, and G. H. Wu, *Appl. Phys. Lett.* **91**, 012510 (2007).

²⁵K. A. Gschneidner, Jr., V. K. Pecharsky, and A. O. Tsokol, *Rep. Prog. Phys.* **68**, 1479 (2005).

²⁶W. B. Pearson, *The Crystal Chemistry and Physics of Metals and Alloys* (Wiley-Interscience, New-York, 1972), pp.146–148.